MULTIFUNCTIONAL NANOCOMPOSITES: SYNTHESIS AND ANTIOXIDANT ACTIVITY ASSESSMENT IN COLLOIDAL DISPERSIONS

VICZIÁN DÁNIEL

University of Szeged, MTA-SZTE "Momentum" Biocolloids Research Group

Abstract

In our environment, there are various highly reactive molecules and ions that can harm both living organisms and industrial products. In living organisms, there are natural defense mechanisms against these harmful substances, including a network of antioxidant enzymes. These enzymes help break down reactive oxygen species (ROS) – which are particularly damaging – therefore they play a crucial role in preventing and treating conditions associated with high ROS levels.

However, these natural enzymes are expensive to produce and they can lose their activity due to small changes in environmental conditions, thus there is a growing need for alternatives. Enzyme-mimicking nanoparticles, i.e., nanozymes, represent a promising alternative due to their low-cost preparation, high durability and tunable physicochemical properties.

Our work focuses on the development of multicomponent materials – composites – with enzyme-like activity. Specifically, we used manganese(IV)-oxide (MnO_2) and cerium(IV)-oxide (CeO_2) nanoparticles, which are known to mimic multiple antioxidant enzymes, such as catalase and superoxide dismutase. Taking into account the conditions under which these nanoparticles operate, we modified their surface charges by attaching a positively charged polymer. This change in surface charge allowed us to create two different composite materials through electrostatic attraction principles. Both composites proved to be remarkably stable as well as able to mimic several antioxidant enzymes, making them promising nanomaterials to be explored in various fields where antioxidants are required.

Introduction

In living organisms and their surroundings, reactive molecules and ions can always be found. A group of these is called reactive oxygen species (ROS), like hydrogen-peroxide (H_2O_2) and superoxide ions ($^{\cdot}O_2^-$). Their accumulation leads to oxidative stress, which is associated with several serious diseases including cancer, diabetes, and cardiovascular conditions. Their production and release are amplified by effects such as alcohol or tobacco consumption and ever-increasing pollution. A natural line of defense is established by organisms in the form of molecular (e.g., vitamin C, glutathione, etc.) and enzymatic (e.g., catalase (CAT), superoxide dismutase (SOD), etc.) antioxidants. Enzymes are particularly effective due to their catalytic function, which means that they are not consumed during the decomposition of ROS. By nature, they are highly relevant materials for applications in various industrial fields, such as the pharmaceutical, food, and textile industries [1]. However, these applications are limited by several inherent drawbacks of natural enzymes. Their extraction, purification, and storage are expensive processes and when external conditions (e.g., pH, temperature, ionic strength, etc.) lie outside their optimal operating window, their activity may be lost completely [2].

There is a strong demand for suitable alternatives to natural enzymes. Among the promising candidates are nanozymes [3] [4], which are nanoparticles with enzyme-like activity. Their advantages include low cost, tunable physicochemical properties, and the ability to remain active under harsh conditions. The main challenge associated with nanozymes is the maintenance of their colloidal stability. Based on the Derjaguin-Landlau-Verwey-Overbeek (DLVO) theory [5], two main effects determine colloidal stability. The attractive van der Waals forces – which are significant only at short distances – and the electrostatic repulsion between dispersed charged particles. The decrease in surface charges and the increase in ionic strength both weaken the stabilizing repulsive forces, resulting in aggregation, where the particles attach to each other, thus forming larger particles and decreasing specific surface area. This is an undesirable process as it reduces the catalytic activity of the system.

Materials and Methods

Materials

Chemicals used during the project were acquired from the commercial suppliers VWR, Sigma-Aldrich, Acros Organics and Alfa Aesar and were used without further purification. The MnO_2 [6] and CeO_2 [7] nanoparticles were previously synthesised using commercially available reagents according to procedures reported in the literature.

Electrophoretic Light Scattering (ELS)

ELS provides information about the surface charges of nanoparticles by observing their motion through a known electric field. The obtained quantity is the electrophoretic mobility (μ_e), from which zeta potential (ζ) values can be calculated using the Helmholz-Smoluchowski equation [8]:

$$\mu_e = \frac{\varepsilon \varepsilon_0 \zeta}{\eta} \tag{1}$$

where η is the dynamic viscosity of the medium, ε is the relative permittivity of the medium and ε_0 is the permittivity of vacuum. The laser wavelength was 658 nm, the temperature of the samples was constant at 25 ± 0.2 °C and the applied voltage at 200 V. The below-listed data points are each the average of 8 measurements.

The extent of functionalization and composite formation was effectively monitored using ELS. The stability of the studied systems could also be estimated from these data. According to the DLVO theory [9] and experimental data, a zeta potential of 30 mV is required for a system to be considered stable.

UV-Visible Spectrophotometry

This technique provides information on the ability of samples to absorb light with wavelengths in the near-UV and visible ranges. The obtained quantity is the absorbance (A), which according to the Lambert-Beer equation is directly related to the concentration (c) of the compound absorbing the light:

$$A = \varepsilon l c \tag{2}$$

where ε is the molar extinction coefficient and l is the length of the light path in the sample.

Catalase (CAT) Assay

The CAT enzyme catalyzes the decomposition of hydrogen peroxide (H_2O_2) into water and molecular oxygen. The process can be monitored by UV-Vis spectrophotometry at 240 nm: the disappearance of H_2O_2 can be followed. Phosphate buffer was used to set the pH to 7.0 and the concentration of H_2O_2 was systematically varied between 0 mM and 1 mM. The absorbance was recorded in 1-second increments for 10 minutes. The initial reaction rate was evaluated by the slope of the linear fit of the obtained curve. The Lambert-Beer equation (2) was used to convert the raw absorbance data to concentration values. The values l = 1 cm and ε = 39,4 M^{-1} cm^{-1} were used for the calculations. The initial reaction rate (v_0) was then plotted as a function of H_2O_2 concentration ([S]) and the obtained graph was fitted according to the Michaelis-Menten equation [10]:

$$v_0 = \frac{v_{max} \cdot [S]}{K_M + [S]} \tag{3}$$

where v_{max} is the largest achievable value of v_0, [S] is the concentration of the substrate (in this case H_2O_2) and K_M is the Michaelis-Menten constant ([S] = K_M if $v_0 = 0.5 \cdot v_{max}$).

Superoxide Dismutase (SOD) Assay

SOD-like activity was assessed by the Fridovich-assay [11]. In this process, superoxide ions are generated in situ during the enzyme-mediated oxidation of xanthine to uric acid. Their presence is monitored using an indicator compound, nitro blue tetrazolium chloride (NBT): a blue coloured product is formed upon reaction with superoxide ions. A small amount of blue product is an indication of the presence of an effective antioxidant capable of scavenging superoxide ions before they react with NBT. The color change can be monitored using UV-Vis spectrophotometry.

At a constant pH of 7.0, the concentration of the studied antioxidant varied between 0 and 2 ppm. Absorbance was recorded over a period of 6 minutes. Inhibition (I), which describes the proportion of NBT reduction prevented by the antioxidant, was calculated using the following equation:

$$I = \frac{(\Delta A_0 - \Delta A_s) \cdot 100}{\Delta A_0} \quad (4)$$

where ΔA_s is the change in absorbance of the sample during the measurement period and ΔA_0 is the ΔA_s value for the sample with 0 ppm antioxidant. IC_{50} is the antioxidant concentration if I = 50%. For the sake of accuracy, accepted ΔA_0 values are the average of three measurements.

Results and Discussion

According to the literature at pH 9 MnO_2 [12] and CeO_2 [13] nanoparticles both possess negative surface charges, therefore mixing the two types of particle dispersions would result in no composite formation due to electrostatic repulsion between the similarly charged species. A two-step process was devised to avoid this issue *(Figure 1)*.

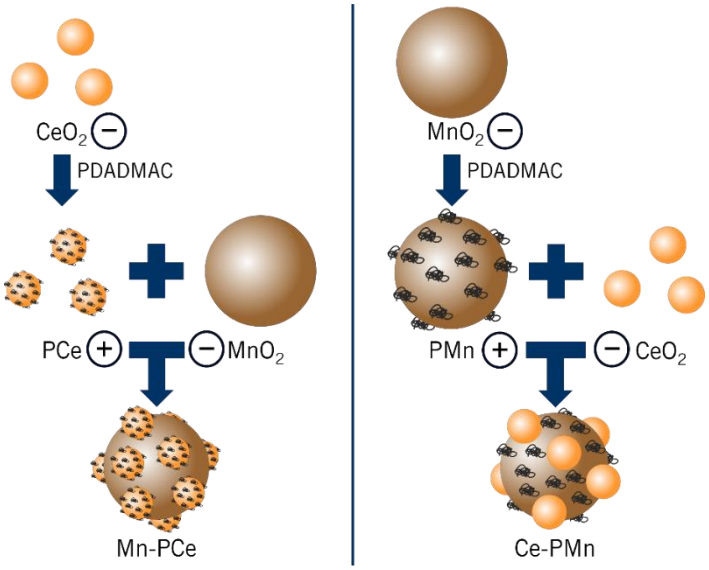

Figure 1: *Schematic overview of composite synthesis*

As the first step, both systems were functionalized using poly-diallyldimethyl-ammonium-chloride (PDADMAC, *Figure 2*) polyelectrolyte: a positively charged polymer. Due to the adsorption of PDADMAC based on electrostatic attraction, the sign of the net surface charge of the particles can be reversed *(Figure 3)*.

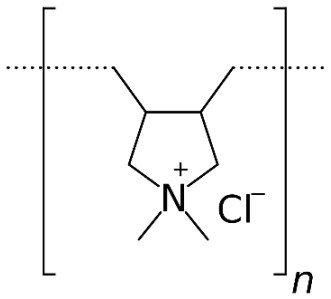

Figure 2: *Structure of PDADMAC*

The concentration of the nanozymes was kept constant while the amount of introduced PDADMAC was systematically varied. At high enough PDADMAC doses charge reversal was observed in both cases. While the low zeta potential at low PDADMAC doses reflects the instability of the bare MnO_2 and CeO_2 dispersions in accordance with the DLVO-theory, at high PDADMAC doses, the zeta potential values indicate a more stable system: functionalization contributed to stability.

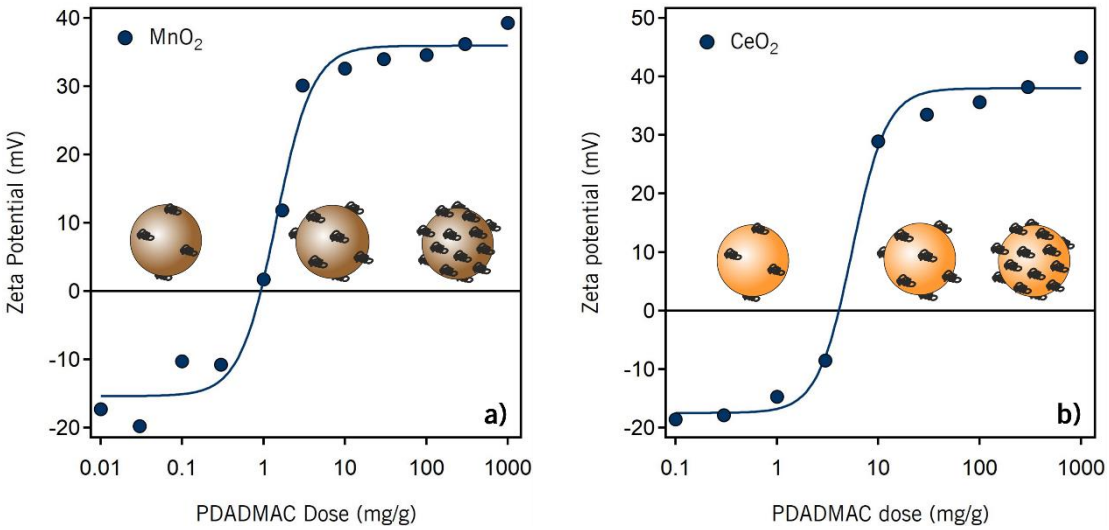

Figure 3: *Functionalization of MnO_2 (a) and CeO_2 (b) nanoparticles*

At this point negatively charged MnO_2 and CeO_2 particles, as well as positively charged, polymer-coated PMn and PCe particles were available to us. Based on the principles of electrostatic attraction, two composites containing both nanozymes can be constructed as outlined in *Figure 1*: mixing CeO_2 and PMn dispersions yielded the Ce-PMn composite *(Figure 4 (a))* while mixing MnO_2 and PCe dispersions yielded the Mn-PCe composite *(Figure 4 (b))*. The process was monitored through ELS.

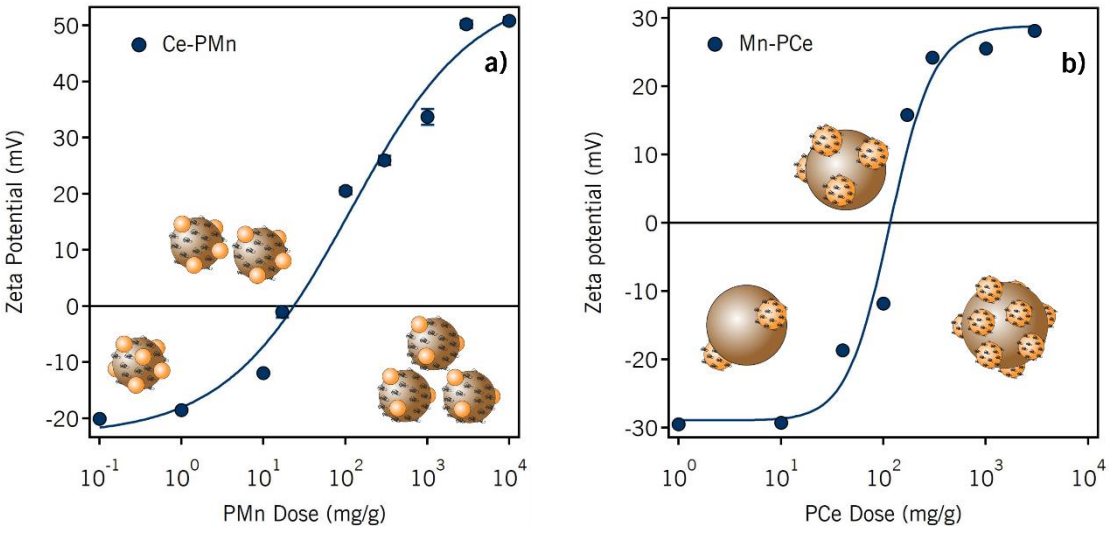

Figure 4: *Formation of Ce-PMn (a) and Mn-PCe (b) composites*

The data show the success of composite synthesis in both cases [14]. The concentration of the bare nanozyme was kept constant while the mass ratio of the two components was systematically varied. At high doses, adsorption of enough positive particles on the surface of negative ones resulted in the overall positive surface charge of the composites. To ensure stable composite particles via high zeta potentials, a 1:1 mass ratio (1000 mg/g) was chosen in both cases for later studies.

Further confirmation of composite formation was obtained through STEM-EDX microscopy images *(Figure 5)*.

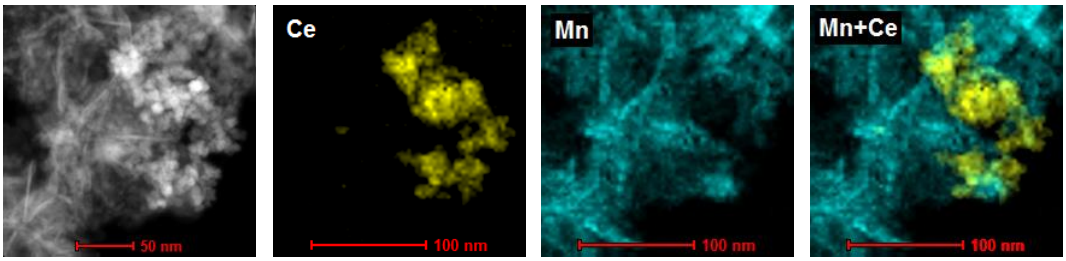

Figure 5: STEM-EDX microscopy images of the Ce-PMn composite

Two types of antioxidant assays were performed with the composites as described above and their results were compared to each other. In the superoxide dismutase assay, achieving 100% inhibition is the optimal goal. Additionally, a minimal concentration of nanozymes required to attain this inhibition level is desired. In the catalase assay, higher reaction rates indicate a more effective system. When visualized graphically, the higher curve in both *Figure 6 (a)* and *Figure 6 (b)* belongs to the better antioxidant.

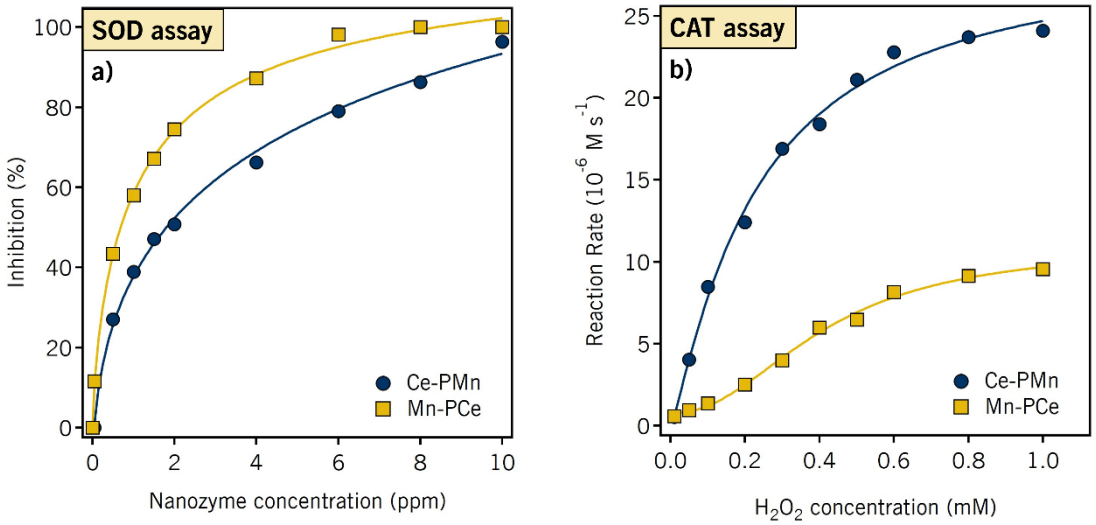

Figure 6: *Comparison of the Ce-PMn and Mn-PCe composites on the SOD (a) and CAT (b) tests*

Based on these results, both composites exhibited significant SOD- and CAT-like activity. The activities can be further quantified and compared using the IC_{50} for the SOD test, as well as K_M and v_{max} values for the CAT test.

System	IC_{50} (SOD)	v_{max} (CAT)	K_M (CAT)
Ce-PMn	1.80 ppm	32.5 ± 1.3 μM s^{-1}	0.29 ± 0.03
Mn-PCe	0.70 ppm	22.6 ± 4.4 μM s^{-1}	1.23 ± 0.37

Table 1: *Summary of the relevant parameters of the SOD and CAT assays*

Out of the two composites, the Mn-PCe was more active as a SOD-mimic: its lower IC_{50} shows that less nanozyme is required to reach 50% inhibition. On the other hand, Ce-PMn proved to be the more effective CAT-mimicking composite: its maximal reaction rate (v_{max}) is higher and the substrate concentration needed to achieve half of v_{max} (K_M) is lower. This inverse relationship hints at a contribution of functionalization: that is the only difference between the two systems.

This project demonstrates the formation of complex composite structures by a simple control of surface charges. The resulting materials proved to mimic multiple antioxidant enzymes effectively, making them promising antioxidants for various industrial applications.

References

[1] O. Kirk, T. Borchert and C. Fuglsang, "Industrial enzyme applications," *Curr. Opin. Biotechnol.,* vol. 13, pp. 345-351, 2003.

[2] X. Ma, A. Hortelão, T. Patiño and S. Sánchez, "Enzyme catalysis to power micro/nanomachines," *ACS Nano,* vol. 10, pp. 9111-9122, 2016.

[3] J. Wu, X. Wang, Q. Wang, Z. Lou, S. Li, Y. Zhu, L. Qin and H. Wei, "Nanomaterials with enzyme-like characteristics (nanozymes): next-generation artificial enzymes (II)," *Chem. Soc. Rev.,* vol. 48, p. 1004, 2019.

[4] M. Zandieh and J. W. Liu, "Nanozymes: Definition, activity, and mechanisms," *Adv. Mater.,* p. 2211041, 2023.

[5] Y. Diao, M. Han, J. Lopez-Berganza, L. Valentino, B. Marinas and R. Espinosa-Marzal, "Reconciling DLVO and non-DLVO forces and their implications for ion rejection by a polyamide membrane," *Langmuir,* vol. 33, pp. 8982-8992, 2017.

[6] H. Chen, J. He, C. Zhang and H. He, "Self-Assembly of Novel Mesoporous Manganese Oxide Nanostructures and Their Application in Oxidative Decomposition of Formaldehyde," *J Phys. Chem. C,* vol. 111, pp. 18033-18038, 2007.

[7] F. Caputo, M. Mameli, A. Sienkiewicz, S. Licoccia and F. Stellacci, "A novel synthetic approach of cerium oxide nanoparticles with improved biomedical activity," *Sci. Rep.,* vol. 7, p. 4636, 2017.

[8] A. Delgado, F. Gonzalez-Caballero, R. Hunter, L. Koopal and J. Lyklema, "Measurement and interpretation of electrokinetic phenomena," *J. Colloid Interface Sci.,* vol. 309(2), pp. 5046-5051, 2007.

[9] B. Derjaguin, "A theory of interaction of particles in presence of electric double-layers and the stability of lyophobe colloids and disperse systems," *Prog. Surf. Sci.,* Vols. 43(1-4), pp. 1-14, 1993.

[10] K. Johnson and R. Goody, "The original Michaelis constant: Translation of the 1913 Michaelis-Menten paper," *Biochemistry,* vol. 50(39), pp. 8264-8269, 2011.

[11] C. Beaucham and I. Fridovich, "Superoxide dismutase - improved assays and an assay applicable to acrylamide gels," *Anal. Biochem.,* vol. 44, pp. 276-287, 1971.

[12] N. B. Alsharif, K. Bere, S. Sáringer, G. F. Samu, D. Takács, V. Hornok and I. Szilágyi, "Design of hybrid biocatalysts by controlled heteroaggregation of manganese oxide and sulfate latex particles to combat reactive oxygen species," *J. Mater. Chem. B,* vol. 9, p. 4929, 2021.

[13] N. B. Alsharif, G. F. Samu, S. Sáringer, A. Szerlauth, D. Takács, V. Hornok, I. Dékány and I. Szilágyi, "Antioxidant colloids via heteroaggregation of cerium oxide nanoparticles," *Colloids Surf. B,* vol. 216, p. 112531, 2022.

[14] N. B. Alsharif, D. Viczián, A. Szcześ and I. Szilágyi, "Formulation of antioxidant composites by controlled heteroaggregation of cerium oxide and manganese oxide nanozymes," *J. Phys. Chem. C,* vol. 127, no. 34, p. 17201–17212, 2023.